

Synthesis of Periodic Mesoporous Coesite

Paritosh Mohanty,[†] Yingwei Fei,[‡] and Kai Landskron*[†]

Department of Chemistry, Lehigh University, Bethlehem, Pennsylvania 18015, and Geophysical Laboratory, Carnegie Institution of Washington, Washington, D.C. 20015

Received April 23, 2009; E-mail: kal205@lehigh.edu

Mesopores are defined as pores with diameters between 2 and 50 nm according to the International Union of Pure and Applied Chemistry.¹ They are in the size regime between micropores (0.3–2 nm) and macropores (>50 nm). While periodic microporous and macroporous materials have been known for many decades and even appear in nature, e.g., in the form of zeolites and opals, the first periodic mesoporous framework, MCM-41, was just discovered in 1992.² MCM-41 was obtained by an astonishingly simple surfactant template-directed “soft assembly” process in aqueous solution.

Nanocasting is a technique that has evolved as an alternative route to periodic mesoporous materials.^{3–7} This method has been shown to be a versatile tool for the synthesis of many periodic mesoporous materials that are not or not easily accessible by soft assembly, for example, carbons and nitrides.^{3–7} Here, a periodic mesoporous framework is used as a so-called “hard template” for the production of a negative replica of the hard template structure.

So far the field of periodic mesoporous frameworks is confined to ambient pressure phases. Porosity and high pressure are antagonists, and a periodic mesoporous high pressure phase seems a contradiction in itself. Therefore, the development of a rational synthesis of periodic mesoporous high pressure phases appeared to us as an intriguing synthetic goal.

Herein, we present the first example of a periodic mesoporous high-pressure phase: Periodic mesoporous coesite. To our best knowledge, this is also the first example of periodic mesoporous silica with crystalline channel walls. Periodic mesoporous organo-silica with partially crystalline channel walls have been discovered by Inagaki et al.⁸ The partial crystallinity in these materials stems from the spatial separation of siliceous and the organic domains inside the channel walls. However, the siliceous domain of these materials remains X-ray amorphous. Inorganic periodic mesoporous materials with crystalline channel walls but compositions other than SiO₂ as well as crystalline mesoporous metal–organic frameworks have also been reported.^{9–12}

The periodic mesoporous coesite has been obtained by a modified nanocasting route from periodic mesoporous silica SBA-16. SBA-16, which was first reported by Stucky et al., has a body centered cubic structure with *Im* $\bar{3}m$ symmetry.¹³ In the first step the SBA-16 mesopores were infiltrated with molten mesophase pitch as a carbon source at its softening point (302 °C) following a modified procedure reported by Ryoo et al.¹⁴ The so-infiltrated pitch was carbonized at 900 °C. The resulting periodic mesostructured silica/carbon composite had negligible surface area and no measurable micro- or mesoporosity according to N₂ sorption. The presence of mesoscale periodicity was checked by small-angle X-ray diffraction, SAXS (Figure S1). The lattice parameter of the composite was found to be slightly reduced after the heat treatment (16.9 vs 18.1

nm). Both the carbon and the silica phase of the SBA-16/C composite were X-ray amorphous according wide-angle X-ray diffraction, WAXS. In the second step the silica/carbon composite was placed into a copper capsule and wetted with three drops of water. The capsule was placed into a large volume multianvil assembly which is described in detail in the Supporting Information (SI). We chose 12 GPa as the synthesis pressure because we considered it high enough to almost certainly allow for a reconstructive transformation into a high pressure phase yet low enough to allow for the synthesis at a convenient scale for characterization of the products by gas sorption. A modest synthesis temperature of 350 °C was chosen to achieve sufficient kinetic activation of the silica phase without deterioration of the mesoscale framework (for experimental details see SI). After decompression and extraction of the sample from the capsule, the sample was subjected to SAXS (Figure S2). The SAXS pattern showed a shoulder around 0.8° 2 θ , which indicates that the mesostructure was preserved during the high-pressure synthesis. The intensity of the reflection peak is reduced in comparison to the starting material, likely due to decreased electronic contrast in the mesostructure.

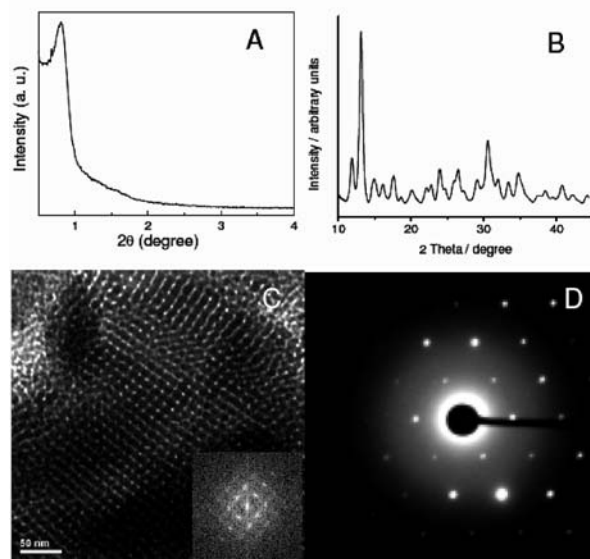


Figure 1. (a) SAXS pattern (Cu K α radiation), (b) WAXS pattern (Mo K α radiation), (c) TEM with FFT image (inset), and (d) SAED of periodic mesoporous coesite.

The product was then heated to 550 °C in air for 5 h to remove carbon. After the treatment the sample appeared white indicating removal of the carbon.

SAXS shows a clear diffraction peak at 0.81° 2 θ demonstrating the high mesoscale periodicity of the product (Figure 1A). The increased intensity of the diffraction peak in comparison to the as-synthesized composite material can be explained by the enhanced

[†] Lehigh University.

[‡] Carnegie Institution of Washington.

electronic contrast. The lattice constant was determined to be 15.4 nm assuming that the mesostructure has retained its cubic symmetry. This is slightly smaller than the lattice constant of the SBA-16/C starting material (16.9 nm). The reduction of lattice constant is plausible considering the high-pressure synthesis conditions and the crystallization of the silica component. WAXS shows resolved reflexes that can be assigned to the coesite structure with unit cell parameters $a = 7.152(5)$ Å, $b = 12.379(5)$ Å, $c = 7.185(2)$ Å, and $\beta = 120.28^\circ$ (Figure 1B).

Transmission electron microscopy (TEM) corroborates that the mesostructure remained in excellent periodic order (Figure 1C). We did not detect any noteworthy amounts of disordered particles or particles without mesostructure. Fourier Transform images (FFT) suggest that the cubic $Im\bar{3}m$ symmetry of the structure is well retained (Figure 1C inset). Selected area electron diffraction (SAED) revealed clearly defined diffraction spots that demonstrate the crystallinity of the channel walls (Figure 1D).

N_2 adsorption at 77 K revealed a type IV isotherm with a steep capillary condensation between $p/p_0 = 0.6$ and 0.75 which is characteristic for periodic mesoporous frameworks (Figure 2). DFT and Monte Carlo analysis of the isotherm revealed a narrow pore size distribution centered around 4.0 nm (Figure 2, inset). The pore sizes are somewhat smaller than those in the original SBA-16 material (5.1 nm). This can be explained by condensation of the silica framework during the carbonization process at 900 °C and silica densification induced by the crystallization process at high pressure. The DFT and Monte Carlo pore size distribution has a small shoulder toward lower pore size that can be interpreted as bottleneck pore entrances that are typical for body centered cubic mesostructures. The desorption branch of the isotherm exhibits a type E hysteresis which is characteristic for mesopore systems with bottlenecks.

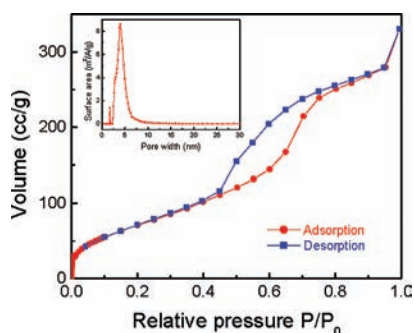


Figure 2. N_2 isotherm of periodic mesoporous coesite. The DFT Monte Carlo pore size distribution is shown as inset.

The BET surface area was determined to be 278 m^2/g . This is smaller than the surface area of the SBA-16 starting material (833 m^2/g). The difference can be explained by the higher crystallinity and density of the coesite channel walls. Higher crystallinity is consistent with reduced mesopore surface roughness and thus reduced surface areas. Furthermore, lower surface areas can be explained by the absence of microporosity in the channel walls of periodic mesoporous coesite. In contrast, microporous channel walls are observed in the SBA-16 starting material and contribute to its surface area (Figure S3). The absence of microporosity in the channel walls of periodic mesoporous coesite is supported by DFT and Monte Carlo analysis of the isotherm. Loss of microporosity during the high pressure treatment is plausible because micropores are unlikely infiltrated by the large mesophase pitch molecules and collapsed during the carbonization step and/or the high pressure

synthesis. The micropore surface areas and the micropore volumes were further calculated by the t-plot method for both the SBA-16 and the periodic mesoporous coesite. While SBA-16 has a considerable micropore surface area of 212 m^2/g and a pore volume of 0.12 cm^3/g , periodic mesoporous coesite revealed a 0.00 m^2/g micropore surface area and 0.00 cm^3/g micropore volume.

The overall pore volume of the periodic mesoporous coesite was determined to be 0.51 cm^3/g . This is only little smaller than the pore volume of the SBA-16 starting material (0.71 cm^3/g). This corroborates that essentially no deterioration of the mesoscale framework occurred during the synthesis of the periodic mesoporous coesite. The small difference can be explained by the elimination of microporosity and the higher framework density of the channel walls.

It is noteworthy that the crystallization process leads to coesite even though stishovite is the thermodynamically stable phase at the chosen pressure and temperature conditions. This phenomenon may be explained by the contributions of surface enthalpy in nanophases that lead to a crossover in stability as the grain size decreases.¹⁵ The alternative is a kinetic crystallization pathway that leads through a coesite intermediate. Due to the mild synthesis temperature the coesite intermediate is stable enough not to convert into stishovite at a significant rate.

We conclude that periodic mesoporous coesite can be made in a two-step nanocasting process: In the first step amorphous silica of an SBA-16/C composite is crystallized at high pressure. In the second step porosity is created by oxidation of the carbon support at ambient pressure. This allows for the following general conclusions: (1) Nanocasting of periodic mesostructures extends extreme pressure conditions. (2) High pressure can be a suitable means to crystallize the channel walls of inorganic mesophases that are difficult to crystallize.

Acknowledgment. We gratefully acknowledge the financial support from Lehigh University and the use of the high pressure facility supported by the Carnegie Institution of Washington. We thank Liwei Deng, Yao Wu, and Li Zhang, for technical assistance.

Supporting Information Available: Materials and methods. Figures S1–S3. Complete ref 11. This material is available free of charge via the Internet at <http://pubs.acs.org>.

References

- (1) Rouquerol, J.; Avnir, D.; Fairbridge, C. W.; Everett, D. H.; Haynes, J. H.; Pernicone, N.; Ramsay, J. D. F.; Sing, K. S. W.; Unger, K. K. *Pure Appl. Chem.* **1994**, *66*, 1739–1758.
- (2) Kresge, C. T.; Leonowicz, M. E.; Roth, W. J.; Vartuli, J. C.; Beck, J. S. *Nature* **1992**, *359*, 710–712.
- (3) Joo, S. H.; Choi, S. J.; Oh, I.; Kwak, J.; Liu, Z.; Terasaki, O.; Ryoo, R. *Nature* **2001**, *412*, 169–172.
- (4) Jun, S.; Joo, S. H.; Ryoo, R.; Kruk, M.; Jaroniec, M.; Liu, Z.; Ohsuna, T.; Terasaki, O. *J. Am. Chem. Soc.* **2000**, *122*, 10712–10713.
- (5) Ryoo, R.; Joo, S. H.; Jun, S. *J. Phys. Chem. B* **1999**, *103*, 7743–7746.
- (6) Kruk, M.; Jaroniec, M.; Ryoo, R.; Joo, S. H. *J. Phys. Chem. B* **2000**, *104*, 7960–7968.
- (7) Lu, A.; Schueth, F. *Adv. Mater.* **2006**, *18*, 1793–1805.
- (8) Inagaki, S.; Guan, S.; Ohsuna, T.; Terasaki, O. *Nature* **2002**, *416*, 304–307.
- (9) Lai, X.; Li, X.; Geng, W.; Tu, J.; Li, J.; Qui, S. *Angew. Chem., Int. Ed.* **2007**, *46*, 738–741.
- (10) Fan, W.; Snyder, M. A.; Kumar, S.; Lee, P.-S.; Yoo, W. C.; McCormick, A. V.; Lee Penn, R.; Stein, A.; Tsapatsis, M. *Nat. Mater.* **2008**, *12*, 984–991.
- (11) Park, Y. K.; et al. *Angew. Chem., Int. Ed.* **2007**, *46*, 8230–8233.
- (12) Qiu, L. G.; Xu, T.; Li, Z. Q.; Wang, W.; Wu, Y.; Jiang, X.; Tian, X. Y.; Zhang, L. D. *Angew. Chem., Int. Ed.* **2008**, *47*, 9487–9491.
- (13) Zhao, D.; Feng, J.; Huo, Q.; Melosh, N.; Fredrickson, G. H.; Chmelka, B. F.; Stucky, G. D. *Science* **1998**, *279*, 548–552.
- (14) Kim, T.; Park, I.; Ryoo, R. *Angew. Chem., Int. Ed.* **2003**, *42*, 4375–4379.
- (15) Navrotsky, A.; Mazeina, L.; Majzlan, J. *Science* **2008**, *319*, 1635–1638.

JA903286M